Supporting Information

Nanoscale Conducting Oxide PlasMOStor

Ho W. Lee[1,2,†], *Georgia Papadakis*[1], *Stanley P. Burgos*[1,2], *Krishnan Chander*[1], *Arian Kriesch*[1,3], *Ragip Pala*[1,2], *Ulf Peschel*[3] *and Harry A. Atwater*[1,2,†]

[1]Thomas J. Watson Laboratories of Applied Physics, California Institute of Technology, United States

[2]Kavli Nanoscience Institute, California Institute of Technology, United States

[3] Inst. of Optics, Information and Photonics & Graduate School in Advanced Optical Technologies, Friedrich-Alexander-University Erlangen-Nuremberg, Germany

[†]Corresponding author e-mail: hwlee@caltech.edu, haa@caltech.edu

Keywords

Plasmonics, transparent conducting oxide, modulator, field-effect modulation, epsilon-near-zero material, nanocircuits, plasmonic slot waveguide, active plasmonics

1. Cross-polarization far-field measurement setup

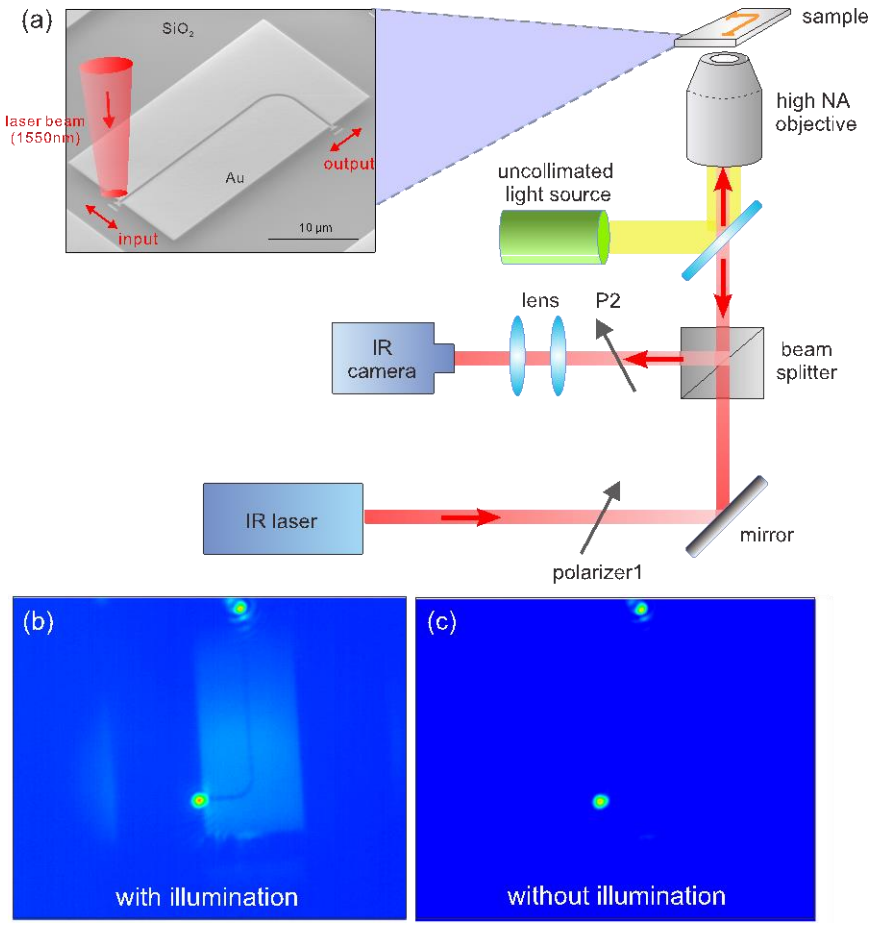

Figure. S1: (a) Schematic of the cross-polarization far-field imaging system used for measuring the plasmon mode properties. Far-field CCD camera image (b) with and (c) without uncollimated light irradiating onto the sample. The input beam is carefully aligned to the nanoantenna for efficient excitation through the illumination scheme.

A high-magnification cross-polarization far-field imaging setup is used for characterizing the optical properties of the propagating plasmonic mode.[1,2] A tunable near infrared laser is directed through a polarizer and a 50/50 non-polarizing beam splitter. The collimated light is then focused using a 100x 0.9 NA microscope objective onto the nanoantenna to excite the gap-plasmon mode of the waveguide (Fig. S1a). The diameter of the collimated beam was measured as FWHM = 1.1 µm using an InGaAs CCD camera and the effective numeric aperture of the experimental focal spot was determined for all subsequent evaluation steps. The output signal is imaged in reflection mode using the infrared camera. Since the waveguide is designed with a 90° bend, the linearly polarized emission from the output of the waveguide is orthogonal to that of the input polarization, thus suppressing back-reflections coming from the incident beam, providing a good signal-to-noise ratio for the desired output signal. An uncollimated

light source together with a thin glass slide are used to irradiate a small amount of light onto the sample for locating the waveguide and antenna positions. As shown in Fig. S1 b,c, the input beam is possible to be aligned precisely to the nanoantenna using a xyz micro-position stage with the illumination scheme.

2. Tunable permittivity of Indium Tin Oxide (ITO)

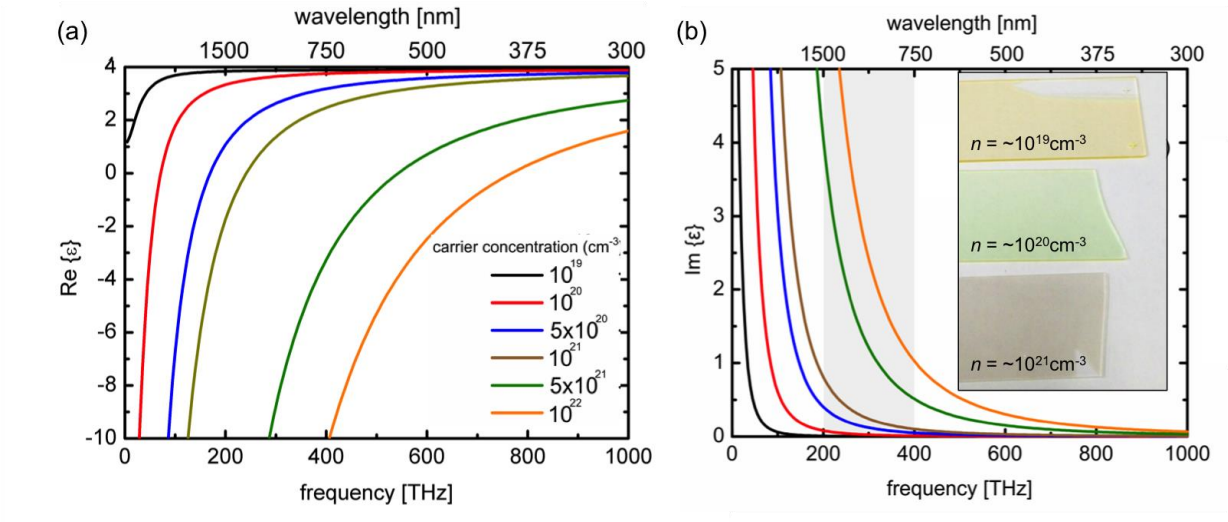

Figure. S2: Calculated complex permittivity of ITO for different carrier concentration of the material using Drude-Lorentz model.

To calculate the tunable permittivity of the ITO material with different carrier concentrations, we use the Drude-Lorentz model as described in the following,

$$\varepsilon = \varepsilon_\infty - \frac{\omega_p^2}{\omega^2 + i\omega\Gamma}$$

$$\omega_p^2 = \frac{ne^2}{\varepsilon_o m^*}$$

where ε is the ITO material permittivity, ε_∞ is the high frequency permittivity (ε_∞ = 3.9 for ITO),[1,2], ε_o is the free space permittivity, ω is the angular frequency in rad/s, ω_p is the plasma frequency, and Γ is the electron scattering rate, m^* is the effective mass (m^*=0.35m_o for ITO, where m_o is the rest mass of electron),[3,4,5] n is the carrier concentration of the ITO, and e is the electron charge.

The calculated complex permittivity of ITO is shown in Fig. S2. It is clear from the figure that the material dispersion shifts significantly to shorter wavelength with higher carrier concentration. The plasma frequencies shift all the way from near-IR (n ~10^{19} cm^{-3}) to UV range (n ~10^{21} cm^{-3}) depending on the carrier concentration of the material. Considering the optical wavelength of λ_0 =1550nm, the real part

of permittivity can tune from positive (dielectric property) to negative (metallic property) with different carrier concentrations, showing the promising tunablility of TCO for tunable plasmonic applications. Note that the carrier concentration of the ITO film can be tuned by changing the fabrication conditions, for instance the oxygen concentration during sputtering. To show the effect, we fabricated different thin films of ITO (thickness = 300nm) onto a silica glass substrate with different sputtering conditions (corresponding to different carrier concentrations of $n \sim 10^{19}$, 10^{20} and 10^{21} cm^{-3}). As seen in the inset of Fig. S2b, different colors are observed from samples due to the different absorption of the materials, indicating the strong tunability with carrier concentration of material. Instead of changing the fabrication condition, we take use the tunable optical properties of TCO by applying a gate voltage to actively change the carrier concentration for developing efficient plasmonic modulation as discussed in the main text.

3. IV measurements for determining the breakdown fields of the oxide layers

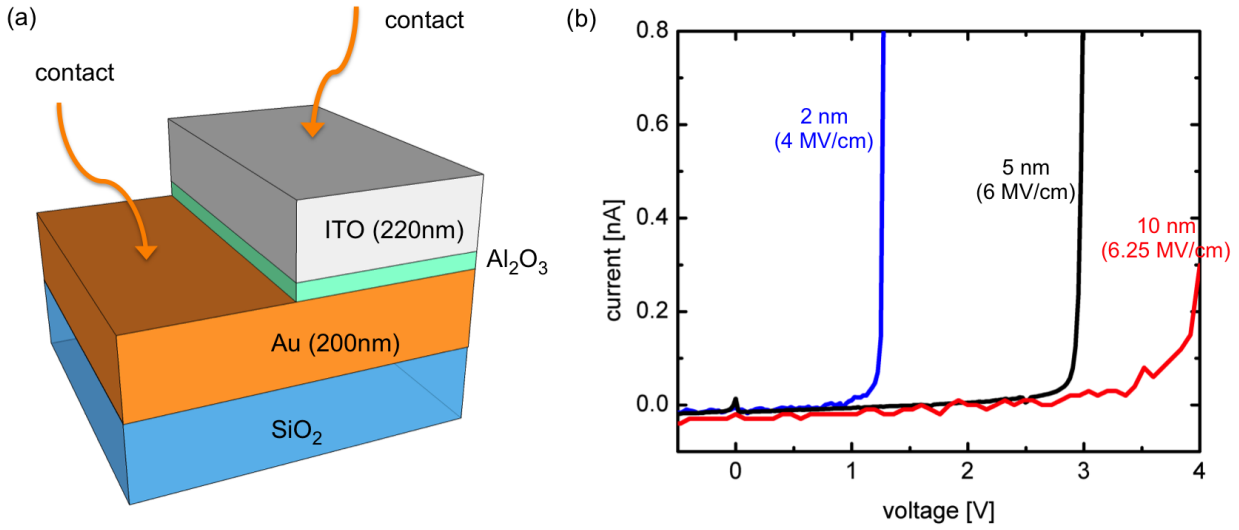

Figure. S3: (a) Schematic of the IV measurement for determining the breakdown fields of different thicknesses of Al_2O_3 insulation layers. (b) Measured IV curves for Al_2O_3 with thickness of 2 nm, 5 nm and 10 nm.

It is important to determine the breakdown voltages for various thicknesses of the Al_2O_3 layer until a current passes between the ITO and gold layers (Fig. S3a). To determine this quantity, a layer of gold (200 nm) is deposited onto a SiO_2 substrate by Ebeam deposition, and an atomic layer deposition (ALD) machine was used to deposit a smooth, thin layer of Al_2O_3 on a small region of the sample (area ~ 4 mm^2, on top of which a layer of ITO (thickness = 220 nm) was placed through sputtering. As shown in Fig. S3a, probes were placed on the gold and ITO layers to produce a voltage difference across the layers and to measure the current. The breakdown voltages, as determined from taking IV measurements for

different Al_2O_3 thicknesses, increase with increasing thicknesses as expected (Fig. S3b). The breakdown electric fields for the 2, 5, and 10 nm layers are 6.25, 6, and 4 MV/cm respectively, which are in the same order of magnitude as the value reported elsewhere.[6] It should be noted that for large area of Al_2O_3 (e.g., > 1 cm^2), there is a possibility of pinholes in the Al_2O_3 from the ALD, thus allowing conductivity between the layers of gold and ITO. With the small waveguide dimension (~ 25 x 25 μm^2) as discussed in the main text (inset of Fig. 3), the Al_2O_3 provided a good electrical insolation, thus field-effect dynamics can be used for efficient modulation.

Reference:

[1] Kriesch, A.; Burgos, S. P.; Ploss, D.; Pfeifer, H.; Atwater, H. A; Peschel, U. *Nano Lett.* **2013**, 13, 4539–4545.

[2] Banzer, P.; Peschel, U.; Quabis, S.; Leuchs, G. *Opt. Express* **2010**, 18, 10905–10923.

[3] Michelotti, F; Dominici, L; Descrovi, E; Danz, N; Menchini, F; *Optics Lett.* **2009**, 34, 839–841.

[4] Bellingham, J. R.; Phillips, W. A.; Adkins, C. J.; *J. Phys.: Condens. Matter* **1990**, 2, 2607-6221.

[5] Neumann, F.; Genenko, Y. A.; Melzer, C.; Yampolskii, S. V.; Seggern, H. V.; *Phys. Rev. B* **2007**, 75, 205322.

[6] Lin, H. C.; Ye, P. D.; Wilk, G. D. *Appl. Phys. Lett.* **2005**, 87, 182904.